

## Computer Simulation of the Distribution of Hexane in a Lipid Bilayer: Spatially Resolved Free Energy, Entropy, and Enthalpy Profiles

Justin L. MacCallum and D. Peter Tieleman\*

Contribution from the Department of Biological Sciences, University of Calgary,  
2500 University Drive NW, Calgary, Alberta T2N 1N4, Canada

Received May 29, 2005; E-mail: tieleman@ucalgary.ca

**Abstract:** The partitioning behavior of small molecules in lipid bilayers is important in a variety of areas including membrane protein folding and pharmacology. However, the inhomogeneous nature of lipid bilayers on a nanometer length scale complicates experimental studies of membrane partitioning. To gain more insight in the partitioning of a small molecule into the lipid bilayer, we have carried out atomistic computer simulations of hexane in a dioleoyl phosphatidylcholine model membrane. We have been able to obtain spatially resolved free energy, entropy, enthalpy, and heat capacity profiles based on umbrella sampling calculations at three different temperatures. In agreement with experiment, hexane partitions preferentially to the center of the bilayer. This process is driven almost entirely by a favorable entropy change, consistent with the hydrophobic effect. In contrast, partitioning to the densest region of the acyl chains is dominated by a favorable enthalpy change with a small entropy change, which is consistent with the “nonclassical” hydrophobic effect or “bilayer” effect. We explain the features of the entropy and enthalpy profiles in terms of density and free volume in the system.

### Introduction

Understanding the partitioning behavior of small molecules in lipid bilayers is an important and difficult problem. Many essential biomolecules such as water, oxygen, and carbon dioxide move across the cell membrane by passive diffusion, which is primarily determined by their partitioning behavior.<sup>1–5</sup> Many drug molecules also enter the cell through passive diffusion across the cell membrane, and thus understanding and fine-tuning their partitioning behavior has important implications for their pharmacokinetics and bioavailability. The mechanism of inhaled anesthetics likely involves membrane ion channels,<sup>6</sup> and the distribution of these molecules within lipid bilayers has been shown to correlate very well with anesthetic potency.<sup>7</sup> Finally, the partitioning behavior of amino acid side chains has important implications in membrane protein folding. Although the partitioning into lipid membranes is often approximated by partitioning between water and olive oil or octanol, a recent study has shown that the free energy of transferring an amino acid from water to the membrane is very different from that of transferring to bulk hydrocarbons, and it has a strong dependence on the depth in the membrane.<sup>8</sup>

The partitioning of a hydrophobic solute from water into a bulk hydrophobic solvent is typically driven by a strongly favorable entropy component and a small enthalpy term, with a large, negative heat capacity change.<sup>9</sup> The hydrophobic effect has traditionally been explained in terms of the ordering of water around a hydrophobic solute, thus the favorable entropy and negative heat capacity change. However, this view has been challenged by the partitioning of some hydrophobic solutes into ordered phases such as lipids<sup>10,11</sup> and high-density reverse-phase chromatography matrices.<sup>9</sup> In these experiments a strong favorable enthalpy is the dominant driving force. The entropic component of the free energy may even be unfavorable in some cases. This phenomenon has been called the “nonclassical” hydrophobic effect or “bilayer” effect.<sup>9–12</sup> Thus, understanding the thermodynamic driving forces for partitioning into inhomogeneous phases such as lipid bilayers is important, yet this question remains largely unresolved.

The distributions of several solutes in lipid bilayers have been determined experimentally. White and co-workers determined, using neutron scattering, that hexane partitions preferentially to the center of dioleoyl phosphatidylcholine (DOPC) membranes.<sup>13</sup> In contrast, halothane<sup>14,15</sup> and ethanol<sup>16</sup> have been

- (1) Bemporad, D.; Essex, J. W.; Luttmann, C. *J. Phys. Chem. B* **2004**, *108*, 4875–4884.
- (2) Bemporad, D.; Luttmann, C.; Essex, J. W. *Biophys. J.* **2004**, *87*, 1–13.
- (3) Marrink, S. J.; Berendsen, H. J. C. *J. Phys. Chem.* **1994**, *98*, 4155–4168.
- (4) Marrink, S. J.; Berendsen, H. J. C. *J. Phys. Chem.* **1996**, *100*, 16729–16738.
- (5) Xiang, T. X.; Anderson, B. D. *Biophys. J.* **1998**, *75*, 2658–2671.
- (6) Eckenhoff, R. G. *Mol. Interventions* **2001**, *1*, 258–268.
- (7) Pohorille, A.; Wilson, M. A.; New, M. H.; Chipot, C. *Toxicol. Lett.* **1998**, *101*, 421–430.
- (8) Hessa, T.; Kim, H.; Bihlmaier, K.; Lundin, C.; Boekel, J.; Andersson, H.; Nilsson, I.; White, S. H.; von Heijne, G. *Nature* **2005**, *433*, 377–381.

- (9) DeVido, D. R.; Dorsey, J. G.; Chan, H. S.; Dill, K. A. *J. Phys. Chem. B* **1998**, *102*, 7272–7279.
- (10) De Young, L. R.; Dill, K. A. *Biochemistry* **1988**, *27*, 5281–5289.
- (11) De Young, L. R.; Dill, K. A. *J. Phys. Chem.* **1990**, *94*, 801–809.
- (12) Wimley, W. C.; White, S. H. *Biochemistry* **1993**, *32*, 6307–6312.
- (13) White, S. H.; King, G. I.; Cain, J. E. *Nature* **1981**, *290*, 161–163.
- (14) Baber, J.; Ellena, J. F.; Cafiso, D. S. *Biochemistry* **1995**, *34*, 6533–6539.
- (15) Eckenhoff, R. G. *Proc. Natl. Acad. Sci. U.S.A.* **1996**, *93*, 2807–2810.
- (16) Feller, S. E.; Brown, C. A.; Nizza, D. T.; Gawrisch, K. *Biophys. J.* **2002**, *82*, 1396–1404.

shown, using NMR and photolabeling experiments, to partition to the interfacial region of the membrane. Lipid bilayers display large gradients in free volume, density, and polarity on very small length scales, making it difficult to determine free energy profiles experimentally. Theoretical approaches, including computer simulation, have proven to be a powerful tool in understanding the hydrophobic effect. Recently much progress has been made in understanding pairwise<sup>17–20</sup> and many-body<sup>21,22</sup> hydrophobic interactions, the size<sup>23–28</sup> and pressure<sup>29</sup> dependence of the hydrophobic effect, and the underlying thermodynamic processes behind the aggregation of hydrophobic solutes in water.<sup>17,30–35</sup> This body of work underscores the utility of theoretical approaches for examining hydrophobic processes that are difficult to study experimentally.

Molecular dynamics (MD) computer simulations have also proven to be very powerful in determining the partitioning of solutes in interfacial systems. Simulations have been able to determine the most favorable location of ethanol<sup>16</sup> and halothane<sup>36</sup> in bilayers. Although excellent agreement with experiment was obtained in both cases, it was not possible to determine the relative free energies for different locations in the bilayer. A number of other studies have used a variety of biased simulation techniques to determine free energy profiles for partitioning a variety of small molecules in a bilayer.<sup>1–4,7,37</sup> Although these studies determined the distribution of small molecules, the thermodynamic driving forces behind these distributions could not be accurately determined.

In this paper we present results from MD computer simulations on the partitioning of hexane into a DOPC bilayer. The calculated distribution is in good agreement with experiment.<sup>13</sup> In addition, we have been able to obtain the free energy, entropy, enthalpy, and heat capacity as a function of depth in the bilayer. These results represent the most detailed view of the partitioning of small molecules into lipid bilayers to date. Although the solute studied is a simple alkane, the results allow us to make predictions for other hydrophobic solvents with slight polar character, and they shed light on the so-called “nonclassical” hydrophobic effect.<sup>12</sup>

- (17) Shimizu, S.; Chan, H. S. *J. Chem. Phys.* **2000**, *113*, 4683–4700.  
 (18) Shimizu, S.; Chan, H. S. *J. Am. Chem. Soc.* **2001**, *123*, 2083–2084.  
 (19) Rick, S. W.; Berne, B. J. *J. Phys. Chem. B* **1997**, *101*, 10488–10493.  
 (20) New, M. H.; Berne, B. J. *J. Am. Chem. Soc.* **1995**, *117*, 7172–7179.  
 (21) Moghaddam, M. S.; Shimizu, S.; Chan, H. S. *J. Am. Chem. Soc.* **2005**, *127*, 303–316.  
 (22) Shimizu, S.; Chan, H. S. *J. Chem. Phys.* **2001**, *115*, 1414–1421.  
 (23) Huang, D. M.; Chandler, D. *Proc. Natl. Acad. Sci. U.S.A.* **2000**, *97*, 8324–8327.  
 (24) Huang, D. M.; Chandler, D. *J. Phys. Chem. B* **2002**, *106*, 2047–2053.  
 (25) Huang, D. M.; Geissler, P. L.; Chandler, D. *J. Phys. Chem. B* **2001**, *105*, 6704–6709.  
 (26) Huang, X.; Margulis, C. J.; Berne, B. J. *Proc. Natl. Acad. Sci. U.S.A.* **2003**, *100*, 11953–11958.  
 (27) Huang, X.; Margulis, C. J.; Berne, B. J. *J. Phys. Chem. B* **2003**, *107*, 11742–11748.  
 (28) Wallqvist, A.; Berne, B. J. *J. Phys. Chem.* **1995**, *99*, 2885–2892.  
 (29) Hummer, G.; Garde, S.; Garcia, A. E.; Paulaitis, M. E.; Pratt, L. R. *Proc. Natl. Acad. Sci. U.S.A.* **1998**, *95*, 1552–1555.  
 (30) Hummer, G.; Garde, S.; Garcia, A. E.; Pratt, L. R. *Chem. Phys.* **2000**, *258*, 349–370.  
 (31) Maibaum, L.; Dinner, A. R.; Chandler, D. *J. Phys. Chem. B* **2004**, *108*, 6778–6781.  
 (32) Hummer, G.; Garde, S. *Phys. Rev. Lett.* **1998**, *80*, 4193–4196.  
 (33) Hummer, G.; Garde, S.; Garcia, A. E.; Paulaitis, M. E.; Pratt, L. R. *J. Phys. Chem. B* **1998**, *102*, 10469–10482.  
 (34) Zhou, R. H.; Huang, X. H.; Margulis, C. J.; Berne, B. J. *Science* **2004**, *305*, 1605–1609.  
 (35) ten Wolde, P. R.; Chandler, D. *Proc. Natl. Acad. Sci. U.S.A.* **2002**, *99*, 6539–6543.  
 (36) Koubi, L.; Tarek, M.; Klein, M. L.; Scharf, D. *Biophys. J.* **2000**, *78*, 800–811.  
 (37) Jedlovsky, P.; Mezei, M. *J. Am. Chem. Soc.* **2000**, *122*, 5125–5131.

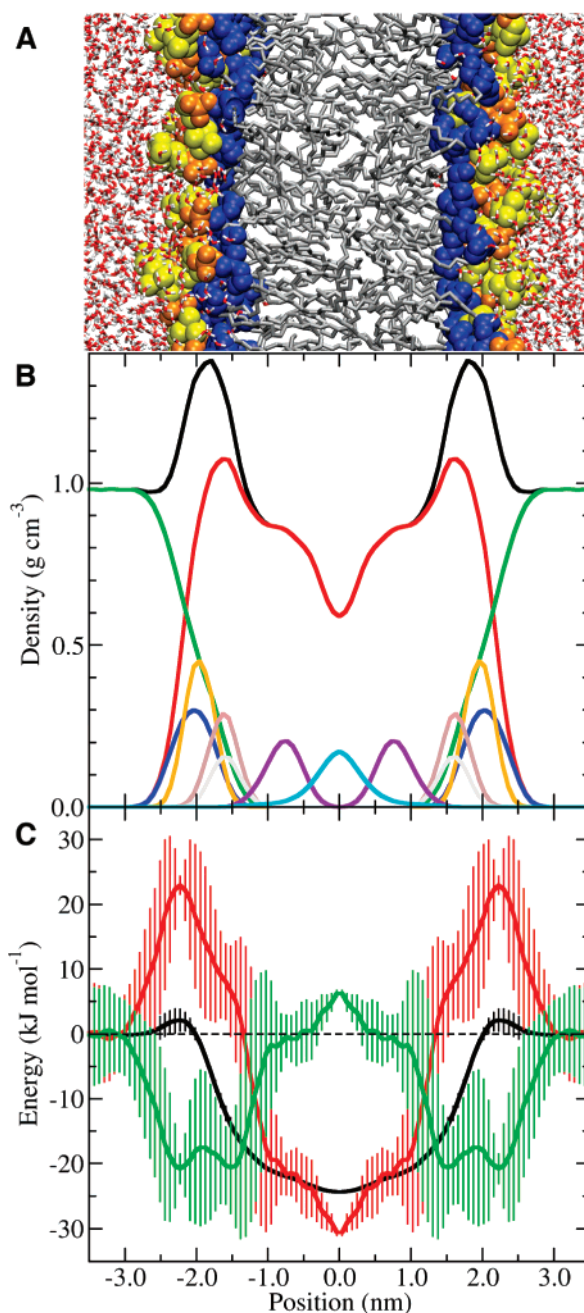


**Figure 1.** Free energy of hexane in a DOPC bilayer. (A) Snapshot of the lipid bilayer system used (red and white tubes, water; yellow spheres, choline; orange spheres, phosphate; blue spheres, glycerol and carbonyl; gray tubes, alkane chains). (B) Average partial density profiles for various functional groups (black, total density; red, lipid; green, water; blue, choline; orange, phosphate; brown, glycerol; gray, carbonyl; purple, double bonds; cyan, methyl). (C) Free energy of partitioning a hexane molecule from bulk water (black, free energy; red, entropic component of free energy,  $-T\Delta S$ ; green, enthalpic component of free energy,  $\Delta H$ ). Vertical bars represent standard errors obtained by measuring the asymmetry between leaflets in the bilayer.

## Methods

A snapshot of the system simulated is shown in Figure 1A. It consists of 64 DOPC molecules, 2807 water molecules, and 2 hexane molecules for a total of 11 892 atoms. Simulations were performed using the GROMACS 3.1 software package.<sup>38,39</sup> The lipids and hexane were

- (38) Berendsen, H. J. C.; van der Spoel, D.; van Drunen, R. *Comput. Phys. Commun.* **1995**, *91*, 43–56.

represented using the force field of Berger et al.,<sup>40</sup> while water was represented using the SPC model.<sup>41</sup> The temperature was controlled using the weak coupling algorithm<sup>42</sup> with a coupling constant of 0.1 ps, while the pressure normal to the bilayer was set to 1 atm with a coupling constant of 1 ps. The area of the system was held at a value of 0.66 nm<sup>2</sup>/lipid, obtained from a previous simulation of pure DOPC under the same conditions. We assume that adding the two hexane molecules does not perturb the area significantly. Bond lengths and angles in water molecules were constrained using the SETTLE algorithm,<sup>43</sup> while all other bond lengths were constrained using the LINCS algorithm.<sup>44</sup> Constraining the bond lengths allowed a time step of 2 fs to be used. The Lennard-Jones interactions were truncated at 1.0 nm. The smooth particle mesh Ewald method<sup>45,46</sup> was used to evaluate the electrostatic interactions, with a real space cutoff of 1.0 nm, fourth-order spline interpolation, and a grid spacing of 0.12 nm.

At equilibrium a hexane molecule will spend only a small amount of time in the water phase compared to the amount of time it spends in the lipid phase. In MD simulations it will be very difficult to obtain accurate statistics about the relative distribution of hexane molecules with reasonable simulation lengths. Free energies obtained from unbiased simulations of 32 hexane molecules in the same bilayer system used here displayed a strong dependence on the starting distribution of hexane molecules, even after 100 ns of simulations (data not shown). To overcome this problem the method of umbrella sampling<sup>47</sup> was used, where an artificial biasing potential is added to force the hexane molecule to sample the region of interest. A series of 25 separate simulations were performed in which the hexane was restrained to a given depth in the bilayer by a harmonic restraint on the *z*-coordinate only. Near the center of the bilayer (from 0.0 to 1.5 nm) and near bulk water (3.0–3.5 nm), a force constant of 500 kJ mol<sup>-1</sup> nm<sup>-2</sup> was used with a spacing of 0.25 nm between the centers of the biasing potentials. For the dense headgroup region (1.5–2.9 nm), a force constant of 3200 kJ mol<sup>-1</sup> nm<sup>-2</sup> was used with a spacing of 0.1 nm between biasing potentials. Two hexane molecules were used, with one per leaflet, allowing additional statistics to be gathered at practically no additional computational cost. Each of the simulations was 20 ns long, for a total of 500 ns per PMF. After the simulations were completed, the unbiased PMF was obtained using the weighted histogram analysis method.<sup>48</sup>

Errors were estimated by measuring the asymmetry of the PMF, which should be zero in the limit of infinite sampling. When using this method, one must choose a point at which the PMFs of each of the two hexane molecules are set equal. We have chosen to make them equal at the center of the bilayer, but this is arbitrary. Our choice of the center of the bilayer means that the uncertainty grows on moving from the center of the bilayer to the water phase. We could also have chosen to make the PMFs equal in the water phase, which would lead to maximum uncertainty in the center of the bilayer. The choice is arbitrary, and the free energy difference and associated uncertainty between any two points is the same regardless of the particular choice. This reflects the nature of PMFs, which really describe the free energy difference between two points along the PMF coordinate, with an associated error for that difference.

The free energy can be decomposed into entropic and enthalpic components through its temperature dependence:

$$-T\Delta S = T\frac{dG}{dT} \approx \frac{T}{2\Delta T}(G(T + \Delta T) - G(T - \Delta T)) \quad (1)$$

$$\Delta H = \Delta G + T\Delta S$$

The umbrella sampling calculations were carried out at three different temperatures (283, 298, and 313 K) and the entropic and enthalpic contributions to the free energy evaluated using eq 1. The heat capacity change was evaluated using

$$\Delta C_p = -T\frac{d^2G}{dT^2} \approx \frac{T}{\Delta T^2}(\Delta G(T - \Delta T) - 2\Delta G(T) + \Delta G(T + \Delta T)) \quad (2)$$

The PMFs at all three temperatures were aligned so that they had a value of zero in the water phase (3.5 nm), and thus all free energies, enthalpies, entropies, and heat capacities are relative to hexane in water.

To further verify the umbrella sampling results, the free energy of transferring a hexane from bulk water to the center of the bilayer was calculated using the thermodynamic integration method. To obtain the free energy of transfer, two sets of simulations were carried out. In one set the hexane molecule was restrained to the center of the bilayer, while the hexane was in bulk water in the other set. The hexane molecule was alchemically transformed into a ghost particle with no interactions with the rest of the system over the course of 21 1-ns simulations for each phase (lipid and water). Each simulation had a fixed value of the coupling parameter between zero (full interactions of hexane with system) and one (hexane does not interact with the rest of the system) in evenly spaced increments. The free energy was evaluated using a soft-core interaction function<sup>49</sup> and a thermodynamic cycle as described in detail in previous work.<sup>50</sup>

The orientational preference of the hexane molecule was quantified by calculating the deuterium order parameter ( $S_{CD}$ ), using the GRO-MACS program *g\_order*. The order parameters were calculated individually for each hexane molecule and the errors estimated from the difference between the two.

## Results and Discussion

A snapshot of the system (Figure 1A) and corresponding partial density profiles (Figure 1B) are shown for orientation along with the PMFs obtained from the simulations (Figure 1C). Clearly hexane partitions preferentially to the center of the bilayer, in good agreement with experiment.<sup>13</sup> The free energy profile is relatively flat from 0.0 nm to around 1.5 nm, where it begins to increase rapidly, consistent with the width of the experimental distribution. The free energy exhibits a maximum in the headgroup region (approximately 2.25 nm) before decreasing slightly and leveling off as water reaches its bulk density. Figure 2 compares the calculated distribution with the one obtained by neutron diffraction. In both cases the hexane is confined to the center of the bilayer. The experimental distribution appears to be somewhat narrower than the one we calculate here. However, the experimental distribution also clearly displays “ringing” due to the truncation of the Fourier series at four orders of diffraction. The truncation artifacts and the fact that the calculated and experimental systems are slightly

(39) Lindahl, E.; Hess, B.; van der Spoel, D. *J. Mol. Modell.* **2001**, *7*, 306–317.

(40) Berger, O.; Edholm, O.; Jahrig, F. *Biophys. J.* **1997**, *72*, 2002–2013.

(41) Berendsen, H. J. C.; Postma, J. P. M.; van Gunsteren, W. F.; Hermans, J., SPC. In *Intermolecular Forces*; Pullman, B., Ed.; Reidel: Dordrecht, 1981; pp 331–342.

(42) Berendsen, H. J. C.; Postma, J. P. M.; DiNola, A.; Haak, J. R. *J. Chem. Phys.* **1984**, *52*, 1695–1697.

(43) Miyamoto, S.; Kollman, P. A. *J. Comput. Chem.* **1992**, *13*, 952–962.

(44) Hess, B.; Bekker, H.; Berendsen, H. J. C.; Fraaije, J. G. E. M. *J. Comput. Chem.* **1997**, *18*, 1463–1472.

(45) Darden, T.; York, D.; Pedersen, L. *J. Chem. Phys.* **1993**, *98*, 10089–10092.

(46) Essmann, U.; Perera, L.; Berkowitz, M. L.; Darden, T.; Lee, H.; Pedersen, L. G. *J. Chem. Phys.* **1995**, *103*, 8577–8592.

(47) Torrie, G. M.; Valleau, J. P. *J. Comput. Phys.* **1977**, *23*, 187–199.

(48) Kumar, S.; Bouzida, D.; Swendsen, R. H.; Kollman, P. A.; Rosenberg, J. M. *J. Comput. Chem.* **1992**, *13*, 1011–1021.

(49) Beutler, T. C.; Mark, A. E.; van Schaik, R. C.; Gerber, P. R.; van Gunsteren, W. F. *Chem. Phys. Lett.* **1994**, *222*, 529–539.

(50) MacCallum, J. L.; Tieleman, D. P. *J. Comput. Chem.* **2003**, *24*, 1930–1935.

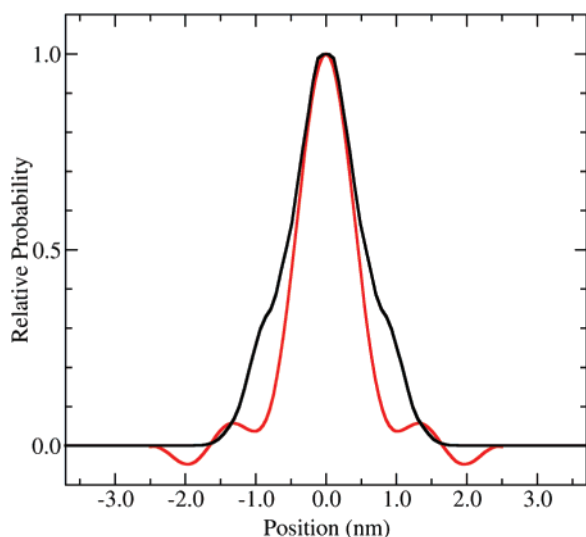


**Figure 2.** Comparison of experimental (red) and calculated (black) distributions of hexane in a DOPC bilayer. Experimental data from ref 13. The two curves have been scaled to coincide at the maximum. The “ringing” and negative density in the experimental profile are due to artifacts from truncating the Fourier series at four orders.

different (high vs low hydration respectively) make a more detailed quantitative comparison impossible.

The umbrella sampling calculations show that the free energy of locating hexane in the center of the bilayer is approximately  $24 \text{ kJ mol}^{-1}$  more favorable than locating it in bulk water. This is consistent with the thermodynamic integration calculations, which yield a value of  $25 \pm 2 \text{ kJ mol}^{-1}$ . If we consider any hexane within 2.5 nm of the bilayer center to be bound to the bilayer, then we can calculate<sup>51</sup> the average free energy for transfer to the bilayer using

$$\Delta G_{\text{W} \rightarrow \text{B}} = -RT \ln \left( \frac{1}{5} \int_{z=-2.5}^{z=2.5} Z(z) \right)$$

where  $z$  is the depth in the bilayer and  $Z(z)$  is the depth-dependent partition function,  $Z(z) = \langle \exp(-G(z)/RT) \rangle$ . This yields a value of  $21 \text{ kJ mol}^{-1}$  for the transfer of hexane from water to the bilayer. The experimental free energy of transfer for a hexane molecule between bulk hexane and water is  $27.3 \text{ kJ mol}^{-1}$ ,<sup>52</sup> while the experimental free energy of transferring hexane from bulk hexane to a low-hydration DOPC bilayer is  $2.5 \text{ kJ mol}^{-1}$ .<sup>13</sup> Thus, the free energy of transferring a hexane from water to the center of a DOPC bilayer is approximately  $27.3 - 2.5 = 24.8 \text{ kJ mol}^{-1}$ , which is consistent with the calculated value.

Figure 3 shows the temperature dependence of the free energy. The shape of the curves is very similar at all three temperatures, although they are clearly different at the center of the bilayer and near the interface. The differences between the curves are small and the uncertainty is relatively high, but we can still calculate the spatially resolved enthalpy and entropy (Figure 1C).

The favorable free energy change of transferring hexane from bulk water to the center of the bilayer (Figure 1C) is driven almost entirely by entropy with only a small enthalpic compo-

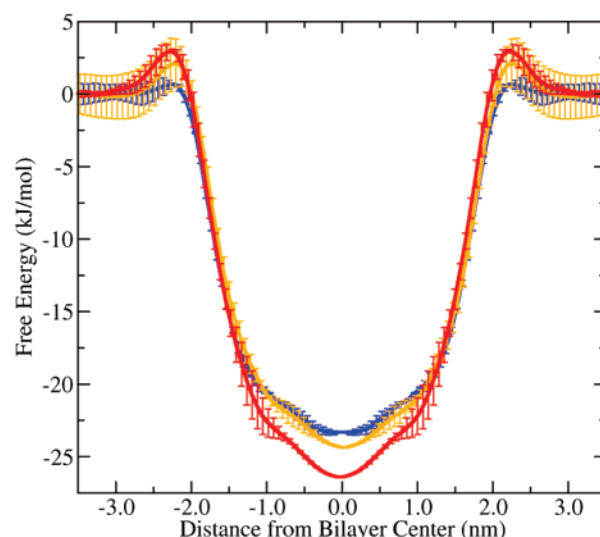


**Figure 3.** Temperature dependence of the free energy. Free energy for transferring hexane from water to a lipid bilayer at 283 (blue), 298 (orange), and 313 K (red). The standard error is indicated with vertical bars.

nent, which is consistent with the hydrophobic effect. Thus, for the partitioning of hydrophobic solutes, the very center of a lipid bilayer appears to have properties very similar to those of a bulk alkane such as octane.<sup>3,53</sup>

Partitioning into the acyl chains becomes increasingly unfavorable on moving from the low-density, unordered region (0.0 nm) to the high-density, highly ordered region ( $\sim 1.4 \text{ nm}$ ). This is driven by opposing trends in the enthalpy and entropy. The enthalpy becomes more favorable while the entropy becomes more unfavorable with increasing acyl chain density.

The fact that the entropy becomes more unfavorable with increasing chain density is consistent with theoretical<sup>3,4,54</sup> and experimental<sup>9–11</sup> results. The increase in entropic free energy with increasing chain density can be understood by examining the changes in acyl chain conformational entropy<sup>54</sup> and the free volume distribution.<sup>3,4,55</sup> Marqusee and Dill<sup>54</sup> have shown through lattice-based statistical mechanical models that adding a solute to the ordered region of the acyl chains decreases the available conformational entropy of the lipid chains and that this decrease becomes more pronounced with increasing chain order. Marrink and co-workers determined that the available free volume in a dipalmitoyl phosphatidylcholine bilayer decreases sharply with the density of the acyl chains.<sup>55</sup> Thus, the probability of finding a pocket of volume large enough to “fit” a hexane molecule will be much larger in the low-density center of the bilayer, and the entropy will therefore be more favorable in the center as well.

The increasingly favorable enthalpy with increasing acyl chain density is explained by the tight packing in the upper portion of the acyl chains. Although the probability of finding a pocket large enough to fit a hexane molecule is low in this region, when a pocket is present the hexane molecule will be packed much more tightly with its surroundings and thus the van der Waals interactions will be more attractive.<sup>4,11,55,56</sup>

(51) Ben-Tal, N.; Honig, B.; Bagdassarian, C. K.; Ben-Shaul, A. *Biophys. J.* **2000**, *79*, 1180–1187.

(52) Lide, D. R. *CRC Handbook of Chemistry and Physics*, 85th ed.; CRC Press: Cleveland, OH, 2004.

(53) Venable, R. M.; Zhang, Y. H.; Hardy, B. J.; Pastor, R. W. *Science* **1993**, *262*, 223–226.

(54) Marqusee, J. A.; Dill, K. A. *J. Chem. Phys.* **1986**, *85*, 434–444.

(55) Marrink, S. J.; Sok, R. M.; Berendsen, H. J. C. *J. Chem. Phys.* **1996**, *104*, 9090–9099.

(56) Xiang, T. X.; Anderson, B. D. *J. Chem. Phys.* **1999**, *110*, 1807–1818.

Due to the presence of two unsaturated chains, DOPC has a relatively large area per lipid, and thus it has a relatively low-density acyl chain region compared to saturated lipids. Also lipids with phosphatidylcholine headgroups generally have larger areas than lipids with other headgroups, such as phosphatidylethanolamine.<sup>57</sup> Experiments using reverse-phase chromatography<sup>9</sup> and experiments that systematically vary the surface density of lipid bilayers<sup>10,11</sup> show that the enthalpy for partitioning becomes increasingly dominant and favorable with increasing surface density, while entropy becomes increasingly less favorable and possibly even unfavorable. Our results show that partitioning to the dense, ordered region of the acyl chains already displays this thermodynamic signature. On the basis of free volume and density arguments, this effect is predicted to become stronger with increasing surface density, explaining the so-called “bilayer” or “nonclassical” hydrophobic effect.<sup>4,12</sup>

Partitioning to the region between the carbonyl groups ( $\sim 1.2$  nm) and the boundary between the lipid and water phases ( $\sim 3$  nm) is dictated by a fine balance between large opposing entropy and enthalpy terms. Partitioning to this region is favored by enthalpy and opposed by entropy. The favorable enthalpy for partitioning to this region is likely due to the high total density in this region, illustrated by the black curve in Figure 1B. The density in this region is much higher than that in the center of the bilayer and is approximately 40% higher than that in bulk water. This region of the bilayer also contains the lowest accessible free volume — even lower than in bulk water.<sup>55</sup> In this region the probability of finding a pocket of volume that a hexane molecule will fit into is very low, and thus there is a strong entropic penalty for partitioning into this region. The fact that the entropy of partitioning into this region is even higher than that of partitioning into bulk water is quite surprising, but it is consistent with experiments measuring partitioning into highly ordered, high-density reverse-phase liquid chromatography columns.<sup>9</sup>

The heat capacity change is an important marker of the hydrophobic effect. There is normally a large negative change in the heat capacity upon transferring a hydrophobic solute from water into an alkane environment. However, DeVido and co-workers have shown that manipulating the surface density of alkyl chains bonded to silica beads can dramatically alter the heat capacity change.<sup>9</sup> The heat capacity change can be altered from a large negative value at low densities to near zero at high surface densities. Wimley and White have studied the heat capacity changes for tryptophan analogues binding to palmitoyloleoyl phosphatidylcholine (POPC) bilayers and found that the heat capacity change was always negative for that system.<sup>12</sup> However, the heat capacity change was significantly smaller (more positive) for partitioning into bilayers than for the bulk alkane cyclohexane. The heat capacity changes obtained from our simulations are shown in Figure 4. The uncertainty in the heat capacity is somewhat high, making quantitative examination challenging. The heat capacity change, however, clearly depends strongly on the position in the bilayer. The center of the bilayer appears to have the most negative heat capacity change, which is consistent with this region being the most similar to bulk alkanes. There is a gradual increase in heat capacity on moving up the chains and into the headgroups, and possibly even a

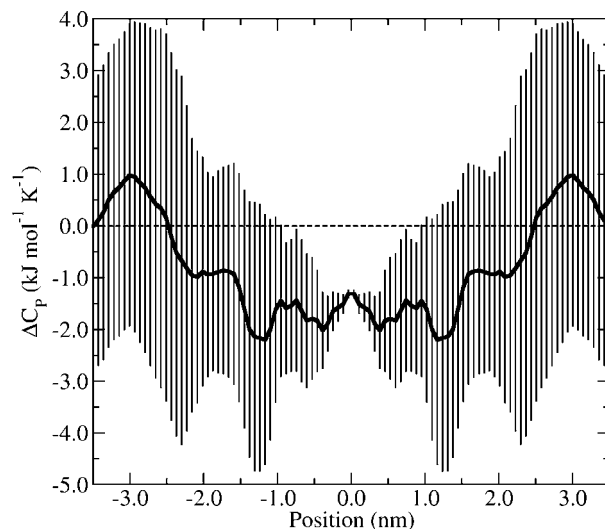


**Figure 4.** Heat capacity change as a function of position for hexane in a DOPC bilayer. Calculated using eq 2. Error bars represent the standard error.

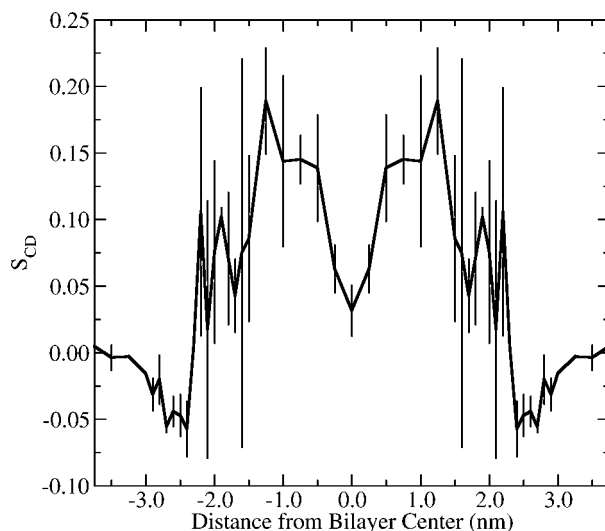


**Figure 5.** Deuterium order parameter ( $S_{CD}$ ) for hexane as a function of position depth within a DOPC bilayer. Vertical bars indicate the standard error.

positive heat capacity change in the water just outside of the headgroups. Despite the significant uncertainties in the heat capacity profile, the results are consistent with experiment. Partitioning into the low-density region of the alkyl chains has a large negative heat capacity change, while partitioning to the denser regions will lead to a less negative change.

Because hexane is a rather anisotropic molecule, its orientation in the different regions of the membrane is of interest. Figure 5 shows the deuterium order parameters for hexane in a DOPC bilayer, averaged over the central four methylene groups. There is very little preferential alignment of the hexane in the center of the bilayer, with order reaching a maximum near the carbonyl groups (ca. 1.5 nm). The order parameter then decreases, reaching a minimum of about  $-0.05$  at a position just exterior to the choline groups. This is interpreted as the hexane having a slight preference to lie flat against the surface of the bilayer to minimize contact with water. Once the hexane is in bulk water, the order parameter decays to zero, indicating isotropic orientation. The average

(57) Nagle, J. F.; Tristram-Nagle, S. *BBA Rev. Biomembr.* **2000**, *1469*, 159–195.

order parameter was evaluated using

$$\langle S_{\text{CD}} \rangle = \frac{\int \exp[-\Delta G(z)/RT] S_{\text{CD}}(z) dz}{\int \exp[-\Delta G(z)/RT] dz}$$

This yields a value of 0.06 for the order parameter, close to the experimentally measured value of 0.04–0.05.<sup>58</sup> Within the lipid chain region the hexane order parameters generally mirror the order of the lipid tails, with ordering increasing on moving toward the headgroups. At the center of the bilayer the hexane shows very little tendency toward preferential orientation, consistent with the very high free volume in this region. In contrast, in the dense portion of the acyl chains the hexane displays a degree of ordering similar to that in the surrounding lipid environment. This behavior is consistent with the idea of hexane packing into small packets of free volume in this region. Additionally, previous MD simulations have shown that the free volume in this region is distributed as elongated voids running parallel to the lipid tails.<sup>55</sup> The uncertainty in the headgroup region becomes significant due to slow orientational correlation times — consistent with the extremely low free volume in this region. Essentially, the hexane becomes trapped in an irregular pocket of free volume between two lipids and takes a relatively long time to reorient or move to another void. Overall, the preferential ordering of hexane is consistent with both experiment and the simple free volume model of partitioning described above.

(58) Jacobs, R. E.; White, S. H. *J. Am. Chem. Soc.* **1984**, *106*, 6909–6912.

## Conclusion

This work has yielded an unparalleled view of the partitioning of a small-molecule solute in a lipid bilayer. The calculated results for hexane in DOPC are in quantitative agreement with experiment and provide spatially resolved free energy, entropy, enthalpy, and heat capacity profiles. Overall, the free energy for partitioning in a lipid bilayer is determined by a remarkably fine balance between large, opposing entropy and enthalpy terms. Only the very center of the bilayer (about 0.5 nm) has the thermodynamic signature of bulk alkane, whereas the lipid chain ordering becomes a dominant factor elsewhere. The exact balance for a particular solute is likely determined by subtle physical and chemical differences between solutes, such as polarity, size, and shape. Although the computational cost of obtaining free energy profiles at different temperatures at sufficient accuracy to determine enthalpy and entropy profiles is high at the moment, we expect that similar calculations on systematic series of small molecules and different lipids will be very fruitful.

**Acknowledgment.** This work is supported by a grant from the Natural Sciences and Engineering Research Council of Canada (NSERC). D.P.T. is an Alberta Heritage Foundation for Medical Research Senior Scholar and Alfred P. Sloan Foundation Fellow. J.L.M. is supported by studentships from NSERC and Alberta Ingenuity. Portions of these calculations were performed on WestGrid computer facilities and the Canadian Internetworked Scientific Supercomputer (CISS3) project. The authors thank Stephen H. White for providing the experimental data for Figure 2.

JA0535099